MODAL MASS ESTIMATION FOR VIBRATION SERVICEABILITY ASSESSMENT OF FOOTBRIDGES

JMW Brownjohn[1]

ABSTRACT

Recent high-profile failures of footbridges to carry pedestrians without excessive and uncomfortable vibration have shown the need for a better understanding of vibration serviceability of structures under pedestrian loads. Failure to predict excessive response may be due to misunderstanding the mechanism of pedestrian loading, but also due to inaccurate response calculations in code-based assessments during design. For a bridge expected to have a low natural frequency this assessment is a dynamic analysis using linear single degree of freedom models requiring realistic estimates of modal frequency, damping, shape and mass. If the design fails and a retrofit is necessary the same parameters are required, but are expected to be estimated to a higher accuracy by full-scale vibration measurement.

Modal mass and modal damping are critical parameters for the assessment process yet are the most difficult to measure experimentally. This paper evaluates procedures for modal mass estimation via two case studies of problematic mass estimation through structural analysis end experiment. As well as traditional forced vibration testing, methods using calibrated footfall excitation are shown to be remarkably effective.

[1] Professor of Structural Engineering
School of Engineering
University of Plymouth
Drake Circus
Plymouth PL4 8AA
United Kingdom
james.brownjohn@plymouth.ac.uk
tel: +44 (0)1752 233673
fax: +44 (0)1752 232638

subject headings:
Bridge
Vibration
Pedestrians
Serviceability
Modal analysis
Mass
Full-scale tests

VIBRATION SERVICEABILITY ASSESSMENT OF FOOTBRIDGES

The lively nature of footbridges, particularly those that are cable supported, has made them a popular subject for research by structural engineers (1,2) an interest enhanced by recent high-profile failures to carry pedestrians comfortably. For Design codes dealing with vibration serviceability of footbridges (3) suggest either to avoid ranges of natural frequencies matching natural walking paces or to check simulated response to walking against frequency-dependent acceleration levels. For example, the UK design code for footbridges, in the form of BD37/01 (4) specifies, for footbridges having fundamental frequencies below 5Hz, the limiting accelerations in terms of natural frequency for a single pedestrian and goes on to show how to estimate both natural frequency and response levels.

As vibration serviceability problems in footbridges are a result of resonance in either one or a very small number of modes of vibration, for the purposes of response calculation it is appropriate to characterize the bridge as one or a few independent single degree of freedom (SDOF) oscillators. Even with the remarkably optimistic assumptions that the loading can be modeled to a high degree of accuracy and that the response can be assessed objectively, there remains the need to identify appropriate values of modal frequency, modal damping ratio and modal mass.

The currently accepted procedure for vibration serviceability assessment involves predicting the steady state structural response $y(t) = \hat{y}\sin(\omega t)$ due to a harmonic or sinusoidal force $p(t) = \hat{p}\sin(\omega t)$ applied to a structure with modal mass m_r, modal damping ζ_r, modal stiffness k_r and modal frequency $\omega_r = k_r / m_r$ for which the peak response amplitude at resonance obtained after an infinite number of load cycles is given by

$$\hat{y} = \hat{p}/2\zeta_r m_r \ . \qquad \text{Equation 1}$$

In the practical case where a finite number of cycles is applied and steady state resonance has not been achieved, a reduction factor is applied to the resonance response, depending on the number of cycles of oscillation (effectively the number of footfalls) that will be applied to the bridge. Account may be also be taken of the mode shape so that it is not necessary to assume the worst case of walking on the spot at midspan.

Clearly, accurate estimates of damping and mass are equally important in estimating resonant response, but in the cases where only a few cycles of excitation are applied or where the mode frequency is so high that resonance could never be established by normal imperfect walking, damping is less relevant. Figure 1 shows the simulated response of a 145,000kg structure with natural frequency 2Hz and 0.4% damping to a 1kN harmonic force applied for 10 seconds, representative of the effect of 20 on-the-spot and perfectly synchronized jumps. Since the damping is low, the force is almost entirely used to increase the kinetic and potential energy of the system by an amount per cycle which, for a given frequency is dependent only on the mass. It is hard to observe any effect of damping in reducing the increment of response for higher amplitudes even though 50% of the peak resonant response has been achieved after 10 seconds.

ESTIMATION OF FREQUENCY, DAMPING AND MODAL MASS

Modal parameter estimation techniques proliferate (5), but for practical application to civil structures, simple and thoroughly validated curve fitting procedures are used. This section summarises their applications.

Resonant build up and logarithmic decrement

For a linear elastic dynamic system with viscous damping, the equations of motion can be de-coupled into SDOF equations such as, for mode *r* having modal amplitude $y_r(t)$:

$$\ddot{y}_r(t) + 2\zeta_r\omega_r\ddot{y}_r(t) + \omega_r^2 y_r(t) = p(t)/m_r \qquad \text{Equation 2}$$

where $\zeta_r = c_r/2m_r\omega_r$, c_r is modal damping and $p(t)$ is force, not necessarily harmonic.

The solution of Equation 2 for a unit impulse $\delta(t)$ is the 'impulse response function'

$$y_r(t) = \left(1/m_r\omega_r\sqrt{1-\zeta_r^2}\right)\sin\left(\omega_r\sqrt{1-\zeta_r^2}\right)\cdot e^{-\omega_r\zeta_r t}. \qquad \text{Equation 3}$$

which is the characteristic exponentially decaying sinusoid. The same characteristic is also seen in free decay from resonance or initial deflection and a curve fit of experimentally obtained single mode free decay to Equation 3 yields estimates of frequency and damping. This 'logarithmic decrement' method is regarded as the most accurate damping estimation procedure. Naturally, the free decay signal used must belong to the single mode being studied and while such signals can be recovered by processing of a wideband response signals, the most satisfactory origin is the physical free decay of a structure in the one single mode following either resonance or carefully controlled initial conditions of displacement or velocity.

The solutions of Equation 2 in terms of acceleration and velocity for zero damping and harmonic excitation at resonant frequency $p = \hat{p}\sin(\omega_r t)$ are

$$\ddot{y}_r(t) \approx -(\omega_r\hat{p}t/2m_r)\sin(\omega_r t) \text{ and } \dot{y}_r(t) \approx (\hat{p}t/2m_r)\cos(\omega_r t) \qquad \text{Equation 4}$$

which describe the linearly growing part of the response shown in Figure 1. Equation 4 represents the behaviour of a lightly damped system well enough in the first few cycles, hence if it is possible to drive a system at or very close to resonance, it should be possible to recover the modal mass for a curve fit to Equation 4. Even the first half-dozen cycles of response to poorly synchronized forcing can be used to estimate mass.

Relationship between mode shape and modal mass

Structures behaving as SDOF systems with proportional or zero damping adopt characteristic deflected shapes or mode shapes in which inertia and stiffness forces are perfectly balanced in resonance. Mode shapes are described by a modal coordinate ${}^r\psi_j$ giving the amplitude of mode *r* at location *j*. Being an eigenvector, a mode shape has an arbitrary scaling and for purposes of full-scale response studies it is convenient to define a scale by fixing the maximum amplitude over the

structure to be one metre i.e. for maximum amplitude $\left|{}^{r}\psi\right|_{\max} \equiv 1$.

Modal mass is then defined by the product of mass (density) with squared mode shape integrated over the entire structure, i.e. for mode *r*:

$$m_r = \oint {}^{r}\psi^2 dm \qquad \text{Equation 5}$$

If the above scaling is used and the mode shape is largest at point *k*, then for harmonic excitation and response at point *k* in mode *r*, the bridge behaves as a SDOF oscillator with mass m_r. If the force is applied and response measured elsewhere at a point *j* with ${}^{r}\psi_j < 1$ then the modal mass goes with $1/{}^{r}\psi_j^2$ so that it becomes infinite (as expected) at a fixed support. For a uniform linear structure with a perfect half-sine mode shape the modal mass will be exactly half the structure mass.

Frequency response function (FRF) and circle fit

For a SDOF system representing mode *r*, the ratio of acceleration response at location *j* to harmonic force input at location *k* in steady state vibration at frequency ω is defined by the accelerance or inertance form of the FRF having units of mass^{-1}

$$H_{jk}(\omega) = \ddot{Y}_j(\omega)/P_k(\omega) = \frac{{}^{r}\psi_j \, {}^{r}\psi_k}{m_r} \cdot \frac{-\omega^2}{-\omega^2 + \omega_r^2 + 2i\zeta_r\omega_r}. \qquad \text{Equation 6}$$

where $\ddot{Y}_j(\omega)$ is acceleration at location *j*, $P_k(\omega)$ is force at location *k* and ${}^{r}\psi_j \, {}^{r}\psi_k / m_r = {}^{r}A_{jk}$ is the modal constant for the force/response pair *j*,*k*.

The circle fit method (5) is very effective for extracting modal parameters from experimental FRFs when modes are well separated. Where *j*=*k* and ${}^{r}\psi_k = 1$ the 'driving point' modal constant ${}^{r}A_{kk}$ is the inverse of the modal mass m_r and the values of modal constant for fixed driving point and varying *j* provide the mode shape.

Figure 2 shows an example of an experimental FRF of relatively good quality obtained from a floor vibration test using a shaker driven by a broadband chirp signal. Such an experimental FRF is given as real and imaginary data points at discrete and usually evenly spaced frequencies. When plotted in the Nyquist plane, as in the right hand plot of Figure 2, as a sequence of values at increasing frequency, the points rotate about a centre and describe a circle. A resonant frequency shown as a peak in the modulus plot is identified in the Nyquist plot by maximum rotational rate, and the damping ratio is obtained from the relative angle between pairs of data points either side of resonance. For a good circle fit the damping value should be insensitive to choice of data pair, but noisy data result in shifted data points and scatter in damping values. The circle radius can be estimated with relatively high accuracy and its inverse give the product of modal mass and damping, hence errors in damping estimates translate directly to errors in mass estimation. If only the peak resonant response is required (Equation 1) the errors cancel, but as shown in this paper, pure resonance is rarely the concern and when it is, it may not be possible to trust damping estimates obtained from low level shaker tests.

In the example of Figure 2, eight interactive circle fits around the peak at 12Hz provide a mean modal mass of 122,750kg

with standard deviation of 6,200kg, a 5% coefficient of variation. While criteria can be coded for optimal 'best fit' this indicates the level of accuracy achievable for civil structures in well controlled conditions.

PRACTICAL APPLICATION TO TWO BRIDGES

Two experiences are reported where there was a need for but difficulty in obtaining reliable estimation of modal mass. In both cases a range of procedures was adopted, including novel techniques involving direct or indirect measurement of human dynamic loading and parallel estimates of modal mass were obtained from a-priori finite element models.

The first bridge studied (6) is a 140m span shallow steel arch constructed between the parallel tracks of an indoor railway terminus. Figure 3 shows the steel frame during construction and Figure 4 shows the glass-clad end product. The bare frame (skeleton) of the bridge comprises approximately 8×10^5 kg of steel hollow sections clad in an envelope of glass on a steel support frame. According to the consultant, the bridge mass is 6.5×10^3 kg/m i.e. 1.3×10^6 kg total including all fixtures and fittings and includes approximately 2×10^5 kg of glass, although the final value of as-built mass could not be obtained. Following ad-hoc measurements during the final seven months of construction, the bridge was the subject of an unusual analytical and experimental vibration serviceability assessment followed by retrofit based on the results. In particular, accurate estimates of modal frequency mass required for design of a tuned mass damper were obtained from shaker testing and controlled jumping and swaying.

The second bridge (7) is a 46m walkway between two blocks of an educational institution, constructed from open steel frame sections and behaving as a cantilever, with one end connected to the adjoining building only via an elastomeric bearing. The bridge (Figure 5) was studied as part of a continuing investigation into effects of people exciting and controlling flexible structures, and even for such a simple structure the necessary estimation of modal mass was far from simple. Mass estimates were obtained from hammer testing as well as from direct measurement of jumping force and response.

MODAL MASS ESTIMATION FOR STEEL ARCH

Estimation of modal mass from response build up due to jumping

Regardless of modal damping and frequency values, the instantaneous physical change of velocity Δv at a point k on a structure that results immediately from an impulse I applied at point k for which ${}^r\psi_k \equiv 1$ is inversely proportional to m_r i.e.

$$m_r \Delta v = I \,. \qquad \text{Equation 7}$$

The results was put to effect to gauge the modal mass during construction. Figure 6 shows the vertical acceleration response close to the midspan location while a student weighing 720N jumped at a frequency close to that of a mode subsequently identified as the first symmetric vertical mode and designated VS1. This was the first attempt to force vibration by jumping and captured the characteristic of the bridge while it carried a modest non-structural mass of glass cladding. At the time VS1 had a natural frequency of 1.32Hz and the jumping was crudely timed using a stopwatch.

Initially the vibration build up was linear, but with imperfect timing, resonance could not be established, and the response died out. Although the forcing function due to the student was not available, a crude estimate of modal mass could be obtained from simple physical principles. If the weight of the jumper could be concentrated in 'perfect impulses' *I* occurring 1.32 times per second these must have the value *I*=545Ns for to have zero average acceleration. Using equation 7 it follows that for jumping at *f*Hz with weight *W*,

$$\Delta v \approx W / f m_r \ . \qquad \text{Equation 8}$$

Examination of Figure 6 shows that in the early part of the vibration build up before damping has significant effect, peak acceleration increases by 0.0133m/sec^2 per cycle,or Δv =1.61mm/sec in harmonic response, hence $m_r \approx 3.38 \times 10^5$ kg.

The analysis is simplistic and errors must arise from the assumption that the jumping is equivalent to a perfect impulse. The same procedure was reapplied with a jumper weighing 853N when the bridge was structurally complete, and with relatively good prompting possible using metronome, to excite a range vibrations modes involving varying degrees of vertical, torsional and lateral (sway) motion.

Figure 7 upper and lower plots show, respectively, the lateral or vertical response to a sequence of jumping in modes LA1, TS1, VS1, LS1, VA1, TA1 and VS2. The form of these modes is indicated in Figure 8 where L, T and V indicate modes predominantly lateral, torsional or vertical; S and A are symmetric and anti-symmetric and the numeral indicates mode order. Table 1 summarises the exercise with column 6 providing the initial estimate of modal mass for unit mode shape at the jump point using Equation 8.

Improved vertical mode mass estimation from response to jumping

A fixed laboratory force plate was used subsequently to record the vertical forces of the 853N jumper at each of a range of frequencies from 1.1Hz to 3Hz. Figure 9 shows the time series and Fourier amplitudes of vertical force due to jumping at 1.1Hz which is a deliberate (and very tiring) series of individual jumps. Figure 10 shows the same information for jumping at 3Hz, which is much smoother and less tiring. The figures show that jumping at 3Hz more closely resembles a pure sinusoid and that as a result it should be more effective in exciting oscillations at the jumping frequency. Of course the differences depend on individuals. The simple approach using Equation 8 was refined to account for relative effects of real jumping forces compared to the 'equivalent' sequence of periodic and infinitely sharp 'perfect impulses'.

For each jumping frequency the response of an oscillator having the same frequency but unit mass and 1% damping was obtained by numerical simulation of response to 30 seconds of perfect impulses and 30 seconds of recorded real jumping. The ratios of (response to impulses)/(response to real jumping) quantified by RMS and maximum values of the oscillator responses are plotted in Figure 11 which shows that, for example, perfect impulses at 1.1Hz generate three times the response of real jumping i.e. real jumping at this rate is one third as effective as perfect impulses. It also appears that the approximation of

jumping as a perfect impulse is most accurate for jumping around 2Hz, a result that normally be explained in terms of Fourier coefficients. Overestimation of input force corresponds to overestimation of mass, so Figure 11 provides, by interpolation, reduction factors to results from Equation 8 leading to more reliable estimates of modal mass which are given in the last column of Table 1. Since jumping was not at the point of maximum modal response, about 22m from midspan, the mass values for unit maximum mode shape would be smaller.

The low value of m_r for TS1 is remarkable as it shows that even approximately 1.3×10^6kg of steel footbridge can behave as a relatively low mass for a mode with a frequency to match pedestrian gait. Accurate assessment of both damping and mass were thus vital in studying susceptibility to pedestrian-induced response.

Lateral mode mass estimation from response to swaying

A tri-axial laboratory force plate at the National Institute of Education Singapore was used to obtain signals for 'swaying' at two frequencies that would excite bridge lateral modes. Figure 12 shows, as time series and Fourier amplitudes, lateral forces generated during 'swaying' to a 1.8Hz metronome beat, generating signals with 280N amplitude at 0.9Hz and much smaller components at the 3rd and 5th harmonics of this frequency.

A different approach to estimate mass was then used by comparing response build-up measured on the bridge with numerical simulation using the forces of Figure 12 applied to oscillators having unit mass and frequency and damping ratios corresponding to the full-scale modes. The ratio between the simulated and measured responses gives the approximate modal mass values in the last two rows of Table 1 which are subject to tolerance of around 10% corresponding to the degree of repeatability of the swaying forces.

Modal mass estimation from shaker testing

Just before opening the bridge, a forced vibration test of the bridge was conducted using electro-dynamic shakers to define more clearly the modal parameters for all bridge vibration modes up to 3Hz. In the wind-sheltered internal environment of the bridge, the 100N order forces provided by the shakers should have provided an adequate signal to noise ratio. Difficulties in restricting movement of construction workers to the deck meant FRF quality obtained with 204-second chirp excitation was compromised, hence it was possible to estimate natural frequencies and driving point modal masses via circle fitting only for relatively high frequency modes i.e. TS1, LS2 and TA1.

Response during steady state excitation at estimated modal frequencies, illustrated in Figure 13, was used for extracting mode shapes. The shaker frequency did not match the resonant frequency perfectly, but it was still possible to use short initial part of the response build up to estimate mass, the steady state part to estimate mode shape (together with signals from other locations) and the free decay to estimate damping.

Comparison of modal mass estimates

Table 2 presents the modal parameter estimates with the last four columns giving modal mass estimates from four methods. 'FRF' gives values obtained for three modes using the broadband shaker excitation (chirp), 'sine' give values obtained where a clear building up to steady state could be observed as in Figure 13 and 'jump' uses the values from Table 1 corrected to unit maximum modal ordinate. Finally, FEM gives values of modal mass estimated by the consultant's finite element model.

Except the first torsional mode TS1, there is considerable scatter among the values for the same mode. Table 2 also compares experimental and FEM and gives modal assurance criteria (MAC) values that are correlation coefficients between modal ordinates from test and FEM. The frequency matching is reasonable with a consistent FEM overestimation of 8.5% due to either mass or stiffness errors in the modelling. The MAC values show very close correlation between experimental and FEM mode shapes and with the excellent correspondence for mass estimates from TS1 it was finally concluded that the most reliable modal mass values for the design of the tuned mass damper would come from the effectively validated FEM.

MODAL MASS ESTIMATION FOR WALKWAY

A FEM of the walkway (Figure 14), was used to estimate frequencies for 1st lateral, vertical and torsional modes as estimated as L1=0.87 Hz, V1=4.72 Hz and T1=10.23 Hz. Preliminary ambient vibration response shown in Figure 15 indicates strong vertical response around 5Hz with strong lateral response just under 2Hz and also around 4.5Hz. Under the circumstances it is reasonable to assume the peaks correspond to vibration modes, as was confirmed in later forced vibration (hammer) testing. The FEM did not predict the lateral response at all well, yet the vertical mode agreed well in frequency and in mode shape with the cantilevered part participating in pure vertical bending. Strong vertical vibrations of the walkway observed during passage of pedestrians were most likely generated by the third harmonic of footfall forces from those pedestrians moving with pacing rates around 1.67Hz.

Because of the susceptibility to pedestrian excitation, the effect of an on human occupants was studied with respect to move V1 and attempts were made to calibrate human dynamic models indirectly through their effects on dynamic characteristics of the occupied walkway (7). As the effects depend on the relative masses of structure and occupants, an accurate estimate of modal mass was required. From the FEM the modal mass for unit maximum vertical displacement at the free end in this vertical mode was estimated to be 8500kg, about 14% of total mass of the bridge, while for predicted lateral modes involving sway motion of most of the bridge, the FEM indicated masses exceeding 35000kg.

A forced vibration test was carried out using an instrumented hammer to excite vertical or lateral vibrations at the free end. Circle fit (5) was used to estimate modal parameters from the FRFs but with little success as it was difficult to avoid standing on the bridge and affecting the response, difficult to apply a vertical impact at the free end without overloading the accelerometer and difficult to apply a lateral impact. Mode V1 and T1 frequency and damping alone were estimated from the hammer test and mode L1 parameters were estimated from the ambient response data; Table 3 provides the values.

Extensive free decay testing later showed a range of amplitude- (and occupant-) dependent damping values with a representative figure for strong response due to walking being approximately 1.3%.

Modal mass via jumping

With no reliable experimental estimate of modal mass yet available to verify the FEM, a portable force plate was used to estimate mass via direct measurement of contact force together with response at a single point due to a human jumping. The top plot of Figure 16 shows part of the measured acceleration response due to an 80kg student jumping at the free end of the bridge at 2.5Hz to build up a resonant response through the second harmonic of the jumping frequency, at 5Hz. The middle plot shows the force plate signal, and the data were used to estimate modal mass as follows.

For the period up to 62 seconds the measured force signal was used as input to a simulation using Equation 2 with mass m_r=1000kg, $\omega_r = 2\pi \times 5$ Hz and ζ_r =1.3%. The bottom plot of Figure 16 shows the result. For the initial build up, Equation 4 applies and comparison of acceleration increment per cycle between measurement (top plot, 0.08m/sec^2) and simulation (bottom plot, 0.59m/sec^2), leads to an estimate of modal mass m_r=7380kg.

Figure 16 represent a short portion extracted from a three minute of intermittent jumping during which contact force and response were continuously measured. The complete sequence was broken into 16-second frames to create an experimental averaged FRF and the circle fit to the first mode is shown in Figure 17. The frequency and damping agree perfectly with values obtained in free vibration for similar amplitudes so the modal mass estimate of 8130 kg should be reliable.

DISCUSSION

In the last decade there has been rapid development in dynamic testing procedures for civil structures partly driven by a growing demand for their reliable vibration serviceability assessment during design and in service. As the problems occur in structures sensitive to pedestrian movement it is natural that pedestrian loads be used under well controlled conditions to study the problems they cause. This paper presents experiences and techniques where controlled and measured human dynamic loads have been perfectly suited to the situation and have been able to provide modal parameter estimates at least as good as those available from the conventional techniques used in civil experimental studies. Using humans to excite structures for testing is by no means a new idea (1,8,9) but in these case studies calibrated humans have been used (with their complete consent) to identify modal mass, one of the most difficult to measure yet vital parameters necessary for vibration serviceability assessment.

The arch bridge was a learning experience for this form of modal analysis yet it was possible to obtain good modal parameter estimates without resorting to high power and logistically demanding low frequency shakers as used for the much lighter but dynamically similar London Millennium Bridge. The walkway was studied intermittently over a long period in a number of student projects related to vibration control and excitation due to human activity and occupancy, and the portable force plate was found to be a simple and effective transducer.

ACKNOWLEDGEMENTS

The author gratefully acknowledges the opportunities and assistances provided by organisations such as Sheffield University. ARUP, National Institute of Education (PESS) and Land Transport Authority in Singapore, many willing project students, and researchers such as Piotr Omenzetter, Pilate Moyo, Zhang Xin and Tao Nengfu.

APPENDIX. NOTATION

${}^{r}A_{jk}$	modal constant
c_r	modal damping constant
e	2.71828
f	jumping/swaying frequency
$H_{jk}(\omega)$	Frequency response function (FRF)
I	Impulse
k_r	modal stiffness
MAC	Modal assurance criterion
m_r	modal mass
$P_k(\omega)$	Fourier transform of input force
$p(t), \hat{p}$	time dependent and peak input force
W	weight of jumper
$\ddot{Y}_j(\omega)$	Fourier transform of acceleration response
$y(t), \hat{y}$	time dependent and peak displacement response
$y_r(t)$	time dependent modal displacement response
Δv	velocity increment between cycles
${}^{r}\psi_j$	mode shape ordinate
ζ_r	modal damping ratio
ω	circular frequency
ω_r	resonant circular frequency

Subscripts

j	response location
k	force location
r	mode number

REFERENCES

[1] Selberg, A., (1950), *Dampening effect in suspension bridges.* IABSE Publications **10**, 183-198.

[2] Wheeler, J. E., (1982) *Prediction and control of pedestrian-induced vibration in footbridges*., ASCE Journal of Structural Engineering **108**(9), 2045-2065.

[3] Pimentel, R. L., Pavic, A. and Waldron, P., (2001) *Evaluation of design requirements for footbridges excited by vertical forces from walking*' Canadian Journal of Civil Engineering **28**, 769-777.

[4] The Highways Agency (2001), *BD37/01 Steel, concrete and composite bridges: Specifications for loads, Part 2, Appendix C* .

[5] Maia, N. M. M, Silva, J. M. M., He, J., Lieven, N. A. J., Lin, R. M., Skingle, G. W., To, W., and Urgueira, A. P. V., (1997) *Theoretical and Experimental Modal Analysis.* Research Studies Press Ltd.

[6] Roche, M., (2001) *Performance in lieu of prescription in bridge design – Changi Airport mezzanine bridge, Singapore*. Transportation Research Record **1770**, 195-203.

[7] Brownjohn, J. M. W. and Tao, N. F., *Vibration excitation and control of a pedestrian walkway by individuals and crowds*. Submitted to Journal of Sound and Vibration

[8] Glanvill, M. J. and Kwok, K. C. S., (1995) *Dynamic characteristics and wind induced response of a steel frame tower*. Journal of wind Engineering & Industrial Aerodynamics **54/55**, 133-149.

[9] Cherry, S. and Topf, U. A., (1970) Determination of dynamic properties of a tower structure from ambient vibrations, Proceedings. 3rd European Symposium on Earthquake Engineering, Sofia,

FIGURE CAPTIONS

Figure 1 Resonant build up with negligible effect of damping

Figure 2 Example of good quality frequency response function (FRF) for civil structure

Figure 3 Arch bridge: steel frame during construction

Figure 4 View of completed arch bridge with glass cladding

Figure 5 Walkway, with cantilevered end to left

Figure 6 Midspan vertical response to stop-watch timed 72kg student jumping to excite mode VS1

Figure 7 Envelopes of vertical (upper) and lateral (lower) response to prompted jumping to excite modes LA1 (2x), TS1 (3x), VS1, LS1, VA1, TA1 and VS2 in turn

Figure 8 Experimental mode shapes for arch bridge

Figure 9 Time series and Fourier amplitudes of vertical forces for jumping at 1.1Hz

Figure 10 Time series and Fourier amplitudes of vertical forces for jumping at 3Hz

Figure 11 Ratio of response from sequence of 'equivalent' impulses to response from actual loading time series for jumping at frequencies from 1.1Hz to 3Hz.

Figure 12 Lateral forces time series and Fourier amplitudes for 'swaying' with a footfall rate of 1.8Hz

Figure 13 Run up, steady state response due to shaker, and rundown for mode LA1 at 1.47Hz

Figure 14 Isometric View of Finite Element Model of the Bridge

Figure 15 Walkway auto-spectral density of ambient vertical (upper) and lateral (lower) acceleration response

Figure 16 80kg student jumping at 2.5Hz.
top: measured acceleration response
middle: measured contact force
Bottom: simulated acceleration response for 1000kg mass

Figure 17 FRF from data of Figure 16

B

Table 1 Jumping sequence for Figure 7 and modal mass estimates for $\psi_r < 1$

Time	No. of sequences	Jump /sway	Jump rate /Hz	mode	m_r estimate (jump) Δv /cycle (sway)	corrected $m_r/10^3$kg
T=0-300	2	sway	2.92	LA1	0.174mm/sec	575
T=450-650	3	jump	1.63	TS1	337 $\times 10^3$kg	280
T=680-780	1	jump	1.1	VS1	1,653 $\times 10^3$kg	634
T=780-900	1	sway	1.78	LS1	0.28mm/sec	442
T=900-1000	1	jump	1.37	VA1	600 $\times 10^3$kg	392
T=1000:1100	1	jump	2.68	TA1	756 $\times 10^3$kg	577
T=1100-end	1	jump	2.77	VS2.	942 $\times 10^3$kg	720

Table 2 Arch bridge modal parameters from low level vibrations

Mode	Frequency /Hz		MAC	Damping /%	Modal mass /10^3kg			
	Test	FEM			FRF	sine	jump[1]	FEM[2]
LS1	0.891	0.924	0.98	0.43	-	-	314	453
VS1	1.117	1.117	0.99	0.31	-	402	335	480
VA1	1.375	1.574	0.93	0.77	-	543	334	261
LA1	1.465	1.470	0.99	0.39	-	544	348	512
TS1	1.634	1.860	0.99	0.46	160	175	145	147
LS2	2.510	2.750	0.93	0.44	496	-	-	-
TA1	2.701	3.010	0.94	0.30	317	337	422	213
VS2	2.751	3.060	0.65	0.37	-	134	-	312

1 Modal masses corrected to $^{r}\psi_k \equiv 1$ at maximum response

2 Consultant's FEM.

Table 3 Walkway modal parameters from low level vibrations

Mode	Frequency /Hz	Damping /%
V1	4.992	0.85
T1	11.13	1.45
L1	1.962	1.96

Figure 1 Resonant build up with negligible effect of damping

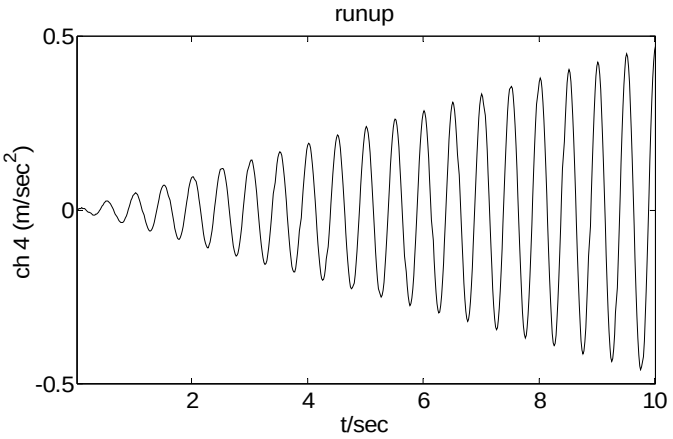

Figure 2 Example of good quality frequency response function (FRF) for civil structure.

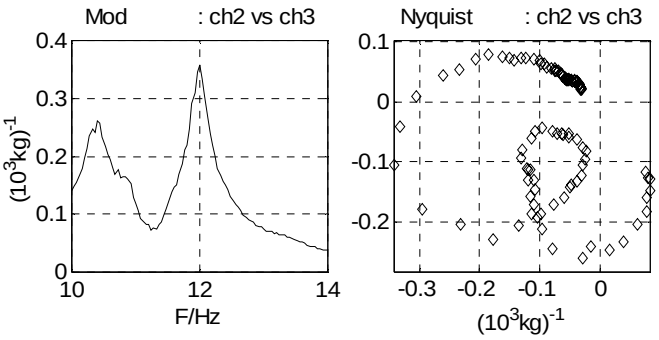

Figure 3 Arch bridge: steel frame during construction

Figure 4 View of completed arch bridge with glass cladding

Figure 5 Walkway, with cantilevered end to left

Figure 6 Midspan vertical response to stop-watch timed 72kg student jumping to excite mode VS1

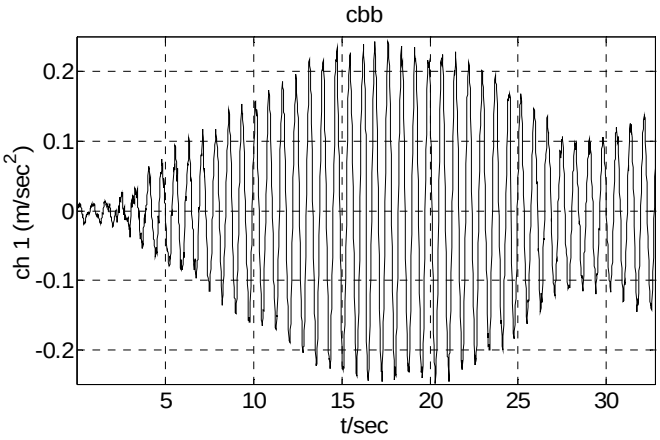

Figure 7 Envelopes of vertical (upper) and lateral (lower) response to prompted jumping to excite modes LA1 (2x), TS1 (3x), VS1, LS1, VA1, TA1 and VS2 in turn

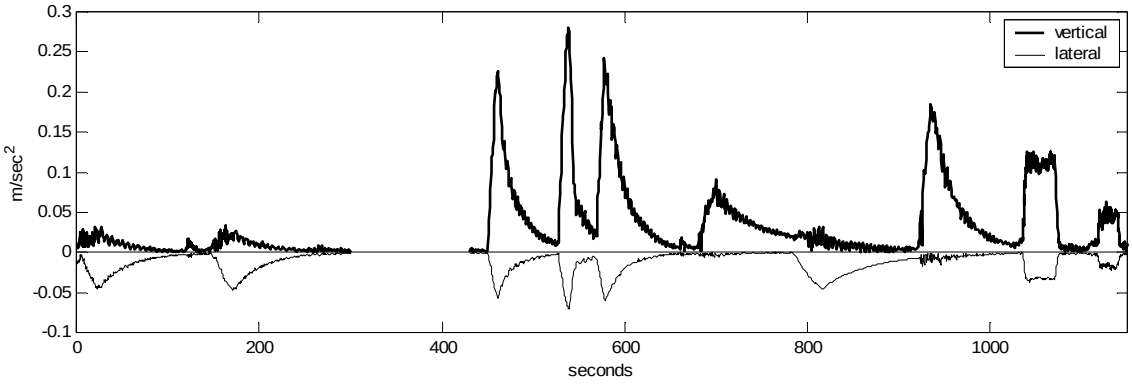

Figure 8 Experimental mode shapes for arch bridge

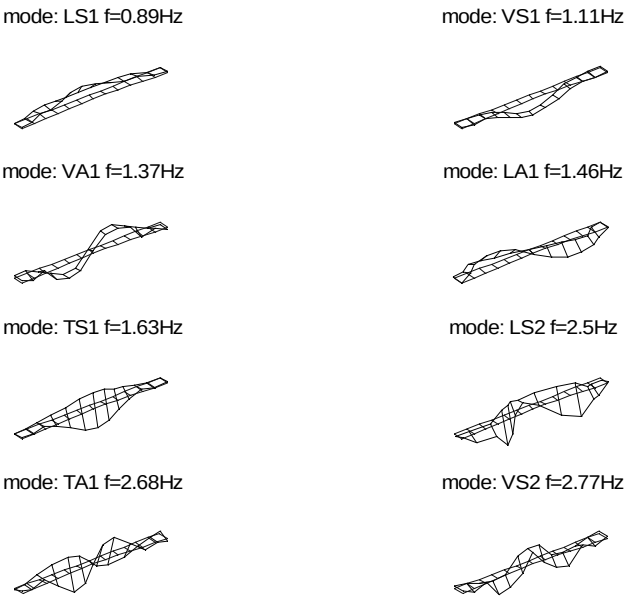

Figure 9 Time series and Fourier amplitudes of vertical forces for jumping at 1.1Hz

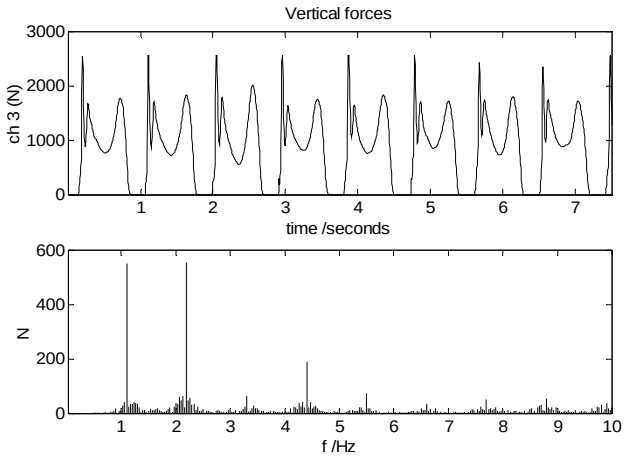

Figure 10 Time series and Fourier amplitudes of vertical forces for jumping at 3Hz

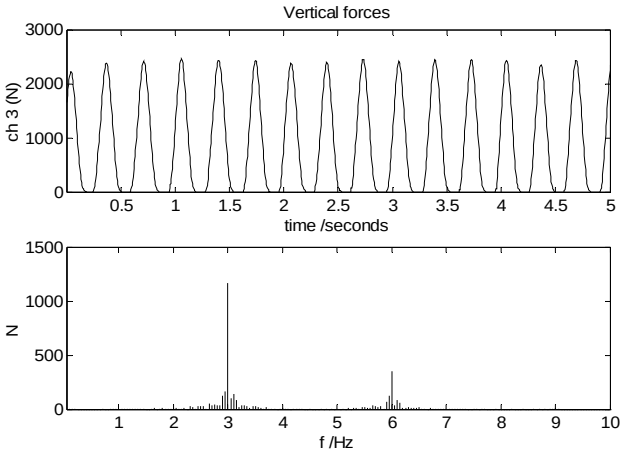

Figure 11 Ratio of response from sequence of ‘equivalent’ impulses to response from actual loading time series for jumping at frequencies from 1.1Hz to 3Hz.

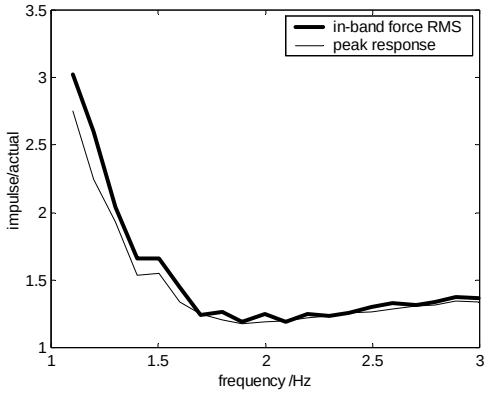

Figure 12 Lateral forces time series and Fourier amplitudes for ‘swaying’ with a footfall rate of 1.8Hz

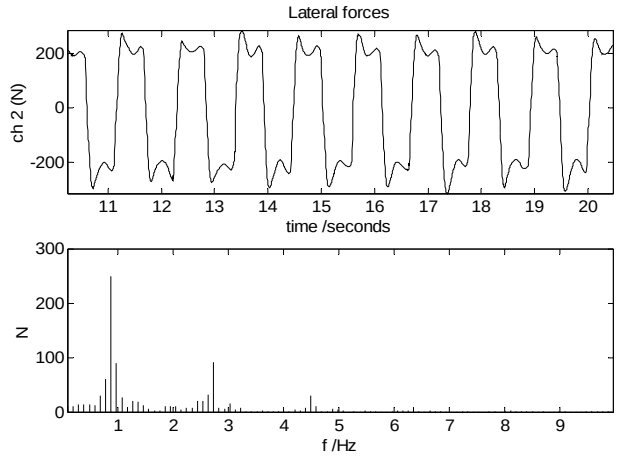

Figure 13 Run up, steady state response due to shaker, and rundown for mode LA1 at 1.47Hz

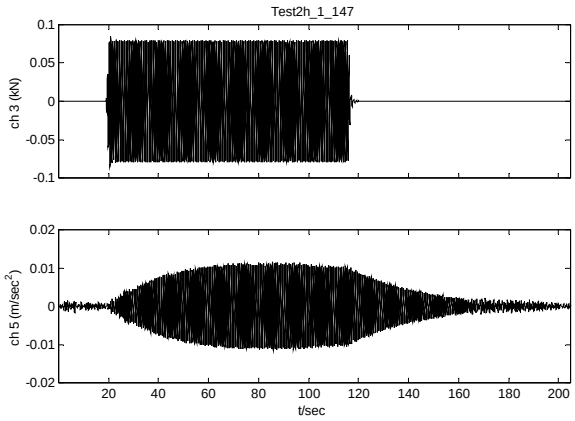

Figure 14 Isometric View of Finite Element Model of the Bridge

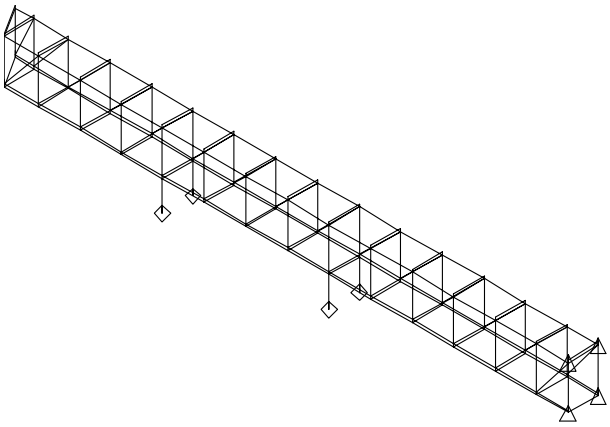

Figure 15 Walkway auto-spectral density of ambient vertical (upper) and lateral (lower) acceleration response

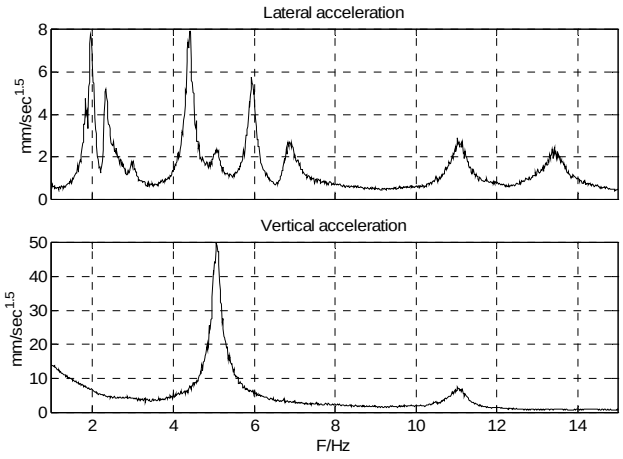

Figure 16 80kg student jumping at 2.5Hz.
top: measured acceleration response
middle: measured contact force
Bottom: simulated acceleration response for 1000kg mass

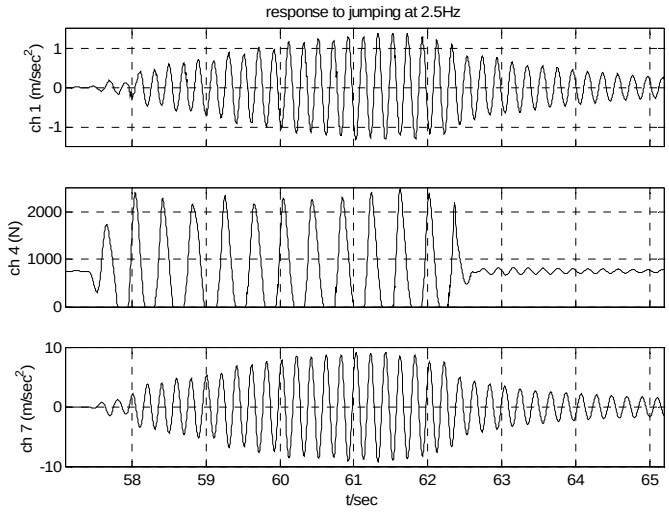

Figure 17 FRF from data of Figure 16